Fermion stars as gravitational lenses

Neven Bilić^{1,2}, Hrvoje Nikolić¹, and Raoul D. Viollier²

ABSTRACT

We study in detail gravitational lensing caused by a supermassive fermion star and compare it with lensing by a black hole of the same mass. It is argued that lensing effects, being very distinct, may shed some light on the yet unexplained nature of the compact dark massive object at the Galactic center.

1. Introduction

Compelling evidence exists (Eckart & Genzel 1996, Genzel et al. 1996, Eckart & Genzel 1997, Genzel et al. 1997, Ghez et al. 1998) that there is a compact dark object of a mass of around $2.6 \times 10^6 M_{\odot}$, concentrated within a radius of ~ 0.015 pc, at the center of the Galaxy, which is usually identified with the enigmatic and powerful radio source Sgr A*. The question whether this is an extended object or a supermassive black hole is still open. Since a compact baryonic object of that mass and size, e.g., a cluster of low-mass stars, is almost excluded, it is worthwhile to explore the possibility of an extended object made of nonbaryonic matter.

In fact, an alternative scenario for supermassive compact dark objects at galactic centers has been developed in the recent past (Viollier et al. 1992, Viollier et al. 1993, Viollier 1994, Tsiklauri & Viollier 1996, Tsiklauri & Viollier 1998a, Tsiklauri & Viollier 1998b, Tsiklauri & Viollier 1999, Bilić et al. 1998, Bilić et al. 1999). In this model, the dark matter at the centers of galaxies is made of nonbaryonic matter in the form of massive neutrinos that cluster gravitationally, forming supermassive neutrino stars in which the degeneracy pressure of the neutrinos balances their self-gravity. Of course, the massive neutrino could be replaced by any weakly interacting fermion of the same mass. Such fermion stars could have been formed in the early Universe during a first-order gravitational phase transition (Bilić & Viollier 1997, Bilić & Viollier 1998, Bilić & Viollier 1999a, Bilić & Viollier 1999b). It has recently been shown that the dark-matter concentration observed through stellar

¹Rudjer Bošković Institute, 10000 Zagreb, Croatia

²Institute of Theoretical Physics and Astrophysics, Department of Physics, University of Cape Town, Rondebosch 7701, South Africa

motion at the Galactic center (Eckart & Genzel 1997, Genzel et al. 1996) is consistent with a supermassive object of 2.5×10^6 solar masses made of self-gravitating, degenerate heavy neutrino matter (Tsiklauri & Viollier 1998a). Moreover, it has been shown that an acceptable fit to the infrared spectrum and the radio spectrum above 20 GHz emitted by matter falling onto the compact dark object, can be reproduced in the framework of standard accretion disk theory (Bilić et al. 1998, Tsiklauri & Viollier 1999) in terms of a baryonic disk immersed in the shallow potential of the degenerate fermion star.

In this paper, we explore possible gravitational lensing effects caused by such an object. Gravitational lensing is a powerful tool which, if observed, yields information on the mass distribution of the lensing object. Wardle & Yusef-Zadeh 1992 suggested that detection of gravitational lensing on a 10 to 100 mas scale might be the signature for Sgr A* being a black hole. If the lensing object is extended and transparent to at least part of the electromagnetic spectrum (baryonic contamination could spoil the transparency to a part of the spectrum), the lensing signal would be quite distinct from that of a black hole. Therefore, if a clear lensing signal is observed around the Galactic center, it could provide a decisive test for the black-hole or fermion-star scenarios. For the sake of comparison, we also present some results for stars made of weakly interacting bosons (Dabrowski & Schunck 1998). These objects are in a way similar to fermion stars, as they consist of matter that interacts mainly gravitationally and therefore is transparent to light, if there is no baryonic contamination. However, boson stars have substantially different scaling properties which make their mass and size negligible compared with stars made of fermions. Even a boson star with maximal mass at a distance comparable with or larger than stellar distances, cannot produce a significant lensing effect unless the boson mass is ridiculously small, e.g., $10^{-10} \text{ eV}.$

This paper is organized as follows: In section 2 we briefly describe the method used and our notation. In section 3 we compare the general features of lensing by a fermion star with those by a boson star or a black hole. In section 4 we investigate lensing effects by a hypothetical compact dark object with properties similar to those at the Galactic center and discuss the possibility of detecting a lensing signal. Our conclusions are given in section 5.

2. Lensing by transparent extended objects

For a static spherically symmetric object, the metric is

$$ds^{2} = e^{\nu(r)}dt^{2} - e^{\mu(r)}dr^{2} - r^{2}(d\vartheta^{2} + \sin^{2}\vartheta d\varphi^{2}). \tag{1}$$

A ray of light, passing at a distance r_0 from the center of the object, is deflected by the angle (Weinberg 1972)

$$\hat{\alpha}(r_0) = 2 \int_{r_0}^{\infty} \frac{dr \ e^{\mu/2}}{\sqrt{\frac{r^4}{h^2}e^{-\nu} - r^2}} - \pi \ , \tag{2}$$

where b is the impact parameter

$$b = r_0 \exp[-\nu(r_0)/2] \ . \tag{3}$$

Let D_{ol} , D_{ls} , and D_{os} denote the distances from the observer to the lens, from the lens to the source, and from the observer to the source, respectively, as depicted in Figure 1. The angular position of the image θ is determined by

$$\sin \theta = b/D_{ol} \tag{4}$$

and (3). The true angular position of the source β is given by the lens equation

$$\beta = \theta - \alpha \,\,\,(5)$$

where α is the reduced deflection angle

$$\alpha(r_0) = \arcsin\left(\frac{D_{ls}}{D_{os}}\sin\hat{\alpha}(r_0)\right) .$$
 (6)

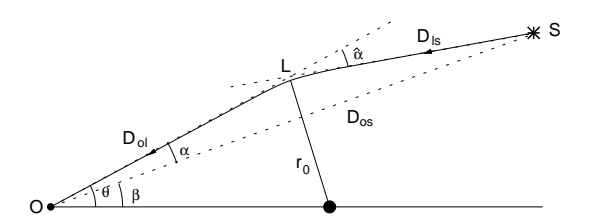


Fig. 1.— Geometry of a gravitational lens system.

The magnification of images is given by (Narayan & Bartelman 1996)

$$\mu = \mu_t \mu_r \,, \tag{7}$$

where μ_t and μ_r are the tangential and radial magnifications, respectively,

$$\mu_t = \frac{\sin \theta}{\sin \beta} , \quad \mu_r = \frac{d\theta}{d\beta} .$$
 (8)

3. Lensing by a Schwarzschild black hole, a boson star, and a fermion star

We first compare gravitational lensing by a fermion star of maximal mass with lensing by a black hole of the same mass and by a boson star of maximal mass. Since fermion and boson stars scale in an essentially different way, we have to choose different natural units in order to make a comparison. The maximal masses of boson and fermion stars are $M_B = 0.63300~M_{\rm Pl}^2/m_B = 8.46 \times 10^{-11} (1\,{\rm eV}/m_B) M_{\odot}$ (Friedberg et al. 1987) and $M_F = 0.38426~\sqrt{2/g} M_{\rm Pl}^3/m_F^2 = 3.43 \times 10^9 \sqrt{2/g} (15\,{\rm keV}/m_F)^2 \,M_{\odot}$ (Bilić & Viollier 1999b), respectively, where m_B is the boson mass, m_F the fermion mass, and $M_{\rm Pl} = \sqrt{\hbar c/G}$ is the Planck mass. The spin-degeneracy factor g is 2 or 4 for Majorana or Dirac fermions, respectively. In the following numerical calculations we take $D_{ls}/D_{os} = 1/2$. Choosing the distance $D_{ol} = 2.41732 \times 10^5$ expressed in units of $\hbar/(cm_B)$, we reproduce the results of Dabrowski & Schunck 1998. In order to obtain comparable lensing caused by a maximal fermion star, we take $D_{ol} = 2.41732 \times 10^5 \, [a]$ for the fermion star, where

$$a = \sqrt{\frac{2}{g}} \frac{\hbar M_{\text{Pl}}}{c \, m_F^2} = 1.3185 \times 10^{10} \sqrt{\frac{2}{g}} \left(\frac{15 \,\text{keV}}{m_F}\right)^2 \,\text{km},$$
 (9)

is the natural length scale for fermion stars (Bilić & Viollier 1999b). We also take the same value D_{ol} for lensing by a black hole. Thus, in our comparison, the mass and the distance expressed in physical units are equal for the fermion star and the black hole, and smaller by a factor $\sqrt{2/g}M_{\rm Pl}m_B/m_F^2$ for the boson star.

The metric outside the black hole is described by the usual empty-space Schwarzschild solution (Weinberg 1972)

$$e^{\nu(r)} = 1 - \frac{2M_F}{r},\tag{10}$$

$$e^{\mu(r)} = \left(1 - \frac{2M_F}{r}\right)^{-1}. (11)$$

For the fermion star the metric is derived by numerically solving Einstein's field equations

$$\frac{d\nu}{dr} = 2\frac{\mathcal{M} + 4\pi r^3 p}{r(r - 2\mathcal{M})},\tag{12}$$

$$\frac{d\mathcal{M}}{dr} = 4\pi r^2 \rho. \tag{13}$$

where the enclosed mass \mathcal{M} is related to the metric by $e^{\mu(r)} = (1 - 2\mathcal{M}(r)/r)^{-1}$, and the pressure p and the density ρ are given by the equation of state for a degenerate relativistic Fermi gas with the metric-dependent Fermi momentum (Bilić et al. 1999, Bilić & Viollier 1999b). For the boson star, the metric is derived by solving equations (12) and (13) coupled with the Klein-Gordon equation for a complex scalar field (Friedberg et al. 1987, Dabrowski & Schunck 1998).

Numerical results are presented in Figures 2 and 3, in which we plot the reduced deflection angle α as a function of the angular position of the image θ . Since the masses and distances are expressed in natural units, the plots are invariant to the choice of g, m_B , and m_F . We note qualitative similarity between lensing by fermion and that by boson stars. In the black-hole case there exists a minimal angular position θ_{\min} corresponding to the impact parameter b_{\min} such that the passing distance r_0 of the light ray equals one and a half Schwarzschild radii R_S . That gives (in natural units) $b_{\min} = \sqrt{27}M_F$, so that $\theta_{\min} = b_{\min}/D_{ol} = 1.7$ arcsec. The function $\alpha(\theta)$ begins to oscillate near the forbidden region between -1.7 and 1.7 arcsec, indicating multiple images appearing approximately 1.5 R_S away from the center. Each oscillation corresponds to a single winding of the light ray around the black hole. In contrast to that, both the boson and the fermion star curves have a smooth transition in the central region. The part of the curve that passes through the center of the plot in Figure 2 corresponds to a secondary image as a result of the ray of light that goes through the object.

4. Lensing by Sgr A*

In this section we study possible lensing effects caused by a supermassive dark object at the center of our galaxy, which we further refer to as Sgr A*. In particular, the trajectories of the images are examined assuming that a lensed star behind Sgr A* moves with a constant velocity, so that its true trajectory passes near the optical axis. We take the central mass to be $M = 2.5 \times 10^6 \ M_{\odot}$, and the distance to it $D_{ol} = 8$ kpc. The compact dark object is modeled as a relativistic degenerate fermion star with the fermion mass $m_F = 15$ keV and the degeneracy factor g = 4. We compare the results of this model with those of the black hole of equal mass. From the observational point of view, the black hole is essentially a pointlike object. On the other hand, the fermion star is an extended object with a nontrivial mass distribution and the radius $R_F = 18.52$ mpc = 0.4775 arcsec.

Let us now assume that a star at a distance D_{ls} behind Sgr A* moves towards the

optical axis with the impact parameter L. We can orient the coordinate system so that the projected velocity v_0 is parallel to the x axis. In Figures 4, 5, 6, and 7 we plot the trajectory of the images for $D_{ls}=200$ pc and for various L ranging from 0.2 to 2 mpc. The dashed circle centered at Sgr A* represents the Einstein ring, the horizontal dashed line describes the true trajectory of the lensed star, and the solid line represents the image trajectories. The image outside the Einstein ring is referred to as primary and those inside as secondary. Figure 4 shows the trajectories of images lensed by the black hole for L=2 mpc. The solid line outside the Einstein ring represents the trajectory of the primary image which begins to deviate substantially from the true trajectory as it approaches the Einstein ring. The trajectory of the secondary image begins at the point $(x=-3R_{\rm S}/2, y=0)$ at the time when the primary image is at infinity on the left. As the star approaches the optical axis and passes to the right, the secondary image makes a loop and finishes at the point $(x=3R_{\rm S}/2, y=0)$ symmetrical to the initial point. In addition to the secondary image, the black hole lens possesses an infinite series of images, very close to the circle of radius $3R_{\rm S}/2$, that are much fainter and practically unobservable.

In contrast to the black hole, which always produces multiple images, a transparent extended object, like a fermion star, may have one, two, or three images depending on L. For L=2 mpc, only one image exists as shown in Figure 5, and its trajectory is similar to the primary image trajectory in the case of black hole. For small values of L, less than 0.2497 mpc, two secondary images will appear at the point A'' corresponding to the position A of the primary image (Figure 7). As the primary image approaches the point B, the two secondary images coalesce and disappear at the point B''. The value L=0.2497 is special as, in that case, the loop made by the two secondary images shown in Figure 7 will degenerate to a very bright single image that will appear (and disappear) when the primary image reaches the top of its trajectory (Figure 6).

One important observable that may significantly differ between the two models of Sgr A* is the velocity of the images. Using simple geometric considerations, we find the square of the image velocity v divided by the projected velocity of the star v_0 in terms of the radial and tangential magnifications

$$(v/v_0)^2 = \mu_r^2 (1 - z^2) + \mu_t^2 z^2, \tag{14}$$

where z is the ratio of the impact parameter to the angular position of the star, $z = L/(\beta D_{os})$. In Figures 8 and 9 we plot the absolute value $|v/v_0|$ as a function of time, assuming that the star moves with the velocity $v_0 = 50 \text{ km/s} = 1.286 \text{ mas/year}$, typical of the velocity of a star in the Galaxy. The behavior of the primary image is similar in the two models, whereas the behavior of the secondary image is different. The secondary image lensed by the black hole (Figure 8) moves in the opposite direction with almost exactly the

same velocity as the primary one. For the fermion star (Figure 9), the time dependence of the velocities of the two secondary images is quite different compared with the velocity of the primary image. Note that during the period of about four years, when all the three images are present, both the primary image and the secondary images are by an order of magnitude faster than the lensed star itself.

In Figures 10 and 11 we plot the total magnification of the images as a function of time. Comparing these figures, one notes two features that are very distinct in the two models. First, for the given set of parameters, the magnifications of the two images lensed by the black hole are almost the same, whereas the magnifications of the images lensed by the fermion star are very different. Second, in the black hole case, the secondary image is slightly fainter than the primary one (Figure 10), as opposed to fermion-star lensing where the secondary images are always brighter (Figure 11). The magnification of the secondary images becomes singular at the points of "creation" A'' and "annihilation" B''.

Next, we investigate the possibility that one of the stars in the vicinity of Sgr A*, e.g., S1 (Eckart & Genzel 1996, Eckart & Genzel 1997) is a lensed image of an object whose true position is behind Sgr A*. I The image of S1 is seen at $\theta_1 = \sqrt{0.19^2 + 0.04^2} = 0.1942$ arcsec = 9.413 × 10⁻⁷ rad (Munyaneza et al. 1998). Since the closest distance between the primary ray of light and the center of the deflecting object is $r_{0(1)} = D_{ol}\theta_1$, we can calculate from (2) the deflection angle of the primary ray. For the black hole, we find $\hat{\alpha}_1 = 6.347 \times 10^{-5}$ rad and for the fermion star, $\hat{\alpha}_1 = 3.264 \times 10^{-5}$ rad. In both cases, $\hat{\alpha}_1 > \theta_1$, implying that in both the black-hole and fermion-star scenarios the extended ray crosses the optical axis behind the lens. The crossing occurs at a distance

$$D_0 = r_{0(1)}/\tilde{\theta} \tag{15}$$

from the center of the lens, where $\tilde{\theta} = \hat{\alpha}_1 - \theta_1$. The true position of the source is somewhere on the extended ray.

In Figures 12 and 13 we present hypothetical lensing of S1. In Figure 12 we fit the two positions observed in 1994 and 1996 (Eckart & Genzel 1997), with a trajectory of the primary image that is close to the Einstein ring, and assuming that no secondary image appears (a situation represented by Figure 5). With only two points, such a fit is, of course, not unique. Our fit is made with the impact parameter L=1 mpc and the distance $D_{ls}=205$ pc. We have made this choice of L and D_{ls} in order to simply demonstrate that a high velocity of one or more objects observed in the vicinity of Sgr A* may be due to lensing. In Figure 13 we show the velocity plot corresponding to the trajectory in Figure 12. The origin is placed at the middle point between 1994.27 and 1996.25. During this period the average projected image velocity of $1660 \pm 400 \text{ km/s}$ has been deduced from the

data (Eckart & Genzel 1997). The true velocity of the star v_0 is smaller by about a factor of eight, hence $v_0 = 200 \pm 50 \text{ km/s}$.

We have to point out that it is very unlikely that the star S1 is indeed a lensed image. The likelihood of such a lensing event may be estimated using the empirical density of stars near the Galactic center (Genzel & Townes 1987):

$$\rho = 2.3 \times 10^5 r^{-1.85} M_{\odot} / \text{pc}^3, \tag{16}$$

where r is the distance from the center in pc. By integrating this density in the tube of radius L = 1 mpc that stretches from $r_1 = 100$ to $r_2 = 300$ pc we find the number of solar masses in that region to be of the order 0.01. Using kinetic theory, the number of stars crossing per unit time into that region can be estimated as

$$\frac{dN}{dt} = \frac{1}{6}\bar{n}\bar{v}\,2\pi L(r_2 - r_1) \tag{17}$$

where $\bar{n} \approx 10 \text{ pc}^{-3}$ is the average star density and $v_0 \approx 50 \text{ km/s}$ the average velocity. This gives a lensing rate of $dN/dt \approx 10^{-4} \text{ yr}^{-1}$. Hence, the probability of observing a lensing event similar to that described above is quite small.

5. Conclusions

We have investigated possible gravitational lensing effects caused by a supermassive dark object made of weakly interacting fermions. Such fermion stars may be alternative candidates for compact dark objects at galactic centers, in particular, at the center of our galaxy referred to as Sgr A*. We have compared lensing effects by Sgr A* in the black hole and fermion star scenarios. We have found a clear distinction between lensing patterns in the two scenarios, assuming the existence of a lensed object that moves close to the optical axis at a distance of about 200 pc behind Sgr A*. We have also investigated the possibility that one of the rapidly moving stars near the Galactic center is a lensed image of an object whose true position is behind Sgr A*.

This work was supported by the Foundation for Fundamental Research (FFR) and the Ministry of Science and Technology of the Republic of Croatia under Contract No. 00980102.

REFERENCES

Bilić, N., Munyaneza, F., & Viollier, R.D. 1999, Phys. Rev. D, 59, 024003

Bilić, N., Tsiklauri, D. & Viollier, R.D. 1998, Prog. Part. Nucl. Phys. 40, 17

Bilić, N., & Viollier, R.D. 1997, Phys. Lett. B 408,75

Bilić, N., & Viollier, R.D. 1998, Nucl. Phys. (Proc. Suppl.) B66, 256

Bilić, N., & Viollier, R.D. 1999a, Gen. Rel. Grav., 31, 1105

Bilić, N., & Viollier, R.D. 1999b, Eur. Phys. J. C, 11, 173

Dabrowski, M.P., & Schunck, F.E., astro-ph/9807039, accepted in ApJ

Eckart, A., & Genzel, R. 1996, Nature, 383, 415

Eckart, A., & Genzel, R. 1997, MNRAS, 284, 576

Friedberg, R., Lee, T.D., & Pang, Y., 1987, Phys. Rev. D35, 3640

Genzel, R., Eckart, A., Ott, T., & Eisenhauer, F. 1997, MNRAS, 291, 219

Genzel, R., Thatte, N., Krabbe, A., Kroker, H., & Tacconi-Garman, L.E. 1996, ApJ, 472, 153

Genzel, R., & Townes, C.H. 1987, ARA&A, 25, 377

Ghez, A.M., Klein, B.L., Morris, M., & Becklin, E.E. 1998, ApJ, 509, 678

Munyaneza, F., Tsiklauri, D., & Viollier, R. D. 1998, ApJ, 509, L105,

R. Narayan, & M. Bartelmann, astro-ph/9606001.

Tsiklauri, D., & Viollier, R.D. 1996, MNRAS, 282, 1299

Tsiklauri, D., & Viollier, R.D. 1998a, ApJ, 500, 591

Tsiklauri, D., & Viollier, R.D. 1998b, ApJ, 501, 486

Tsiklauri, D., & Viollier, R.D. 1999, Astroparticle Phys., 12, 199,

Viollier, R.D., Leimgruber, F.R., & Trautmann, D. 1992, Phys. Lett., B297, 132

Viollier, R.D., Trautmann, D., & Tupper, G.B., 1993, Phys. Lett., B306, 79

Viollier, R.D., 1994, Prog. Part. Nucl. Phys., 32, 51

S. Weinberg, Gravitation and Cosmology, John Wiley & Sons, NY (1972).

Wardle, M., & Yusef-Zadeh, F. 1992, ApJ, 387, L65

This preprint was prepared with the AAS LATEX macros v4.0.

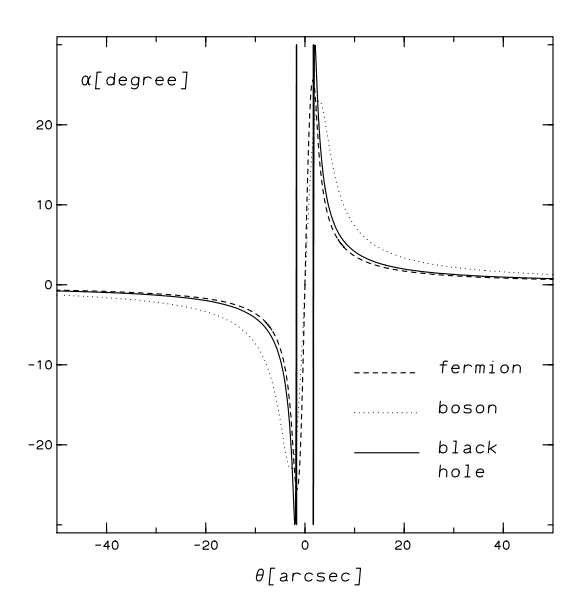


Fig. 2.— Reduced deflection angle versus angular position of the image. The dotted and dashed lines represent the maximal boson and the fermion star, respectively, and the solid line represents a black hole with the same mass as that of the fermion star.

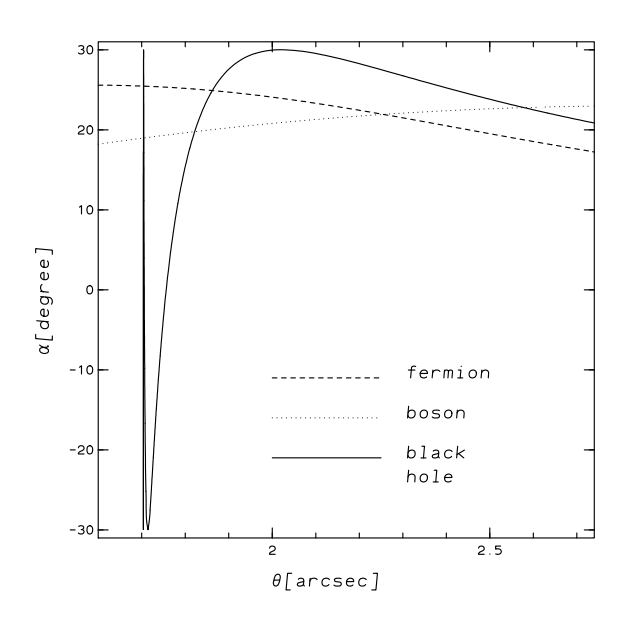


Fig. 3.— Same as in Figure 2, with θ ranging from 1.6 to 2.75 arcsec.

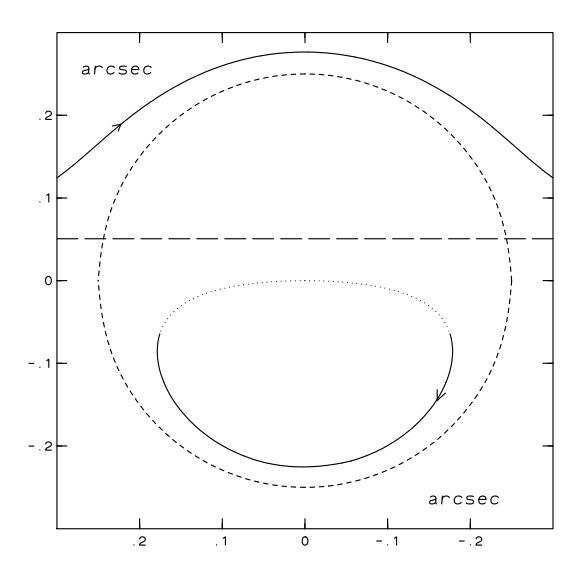


Fig. 4.— Trajectories of the primary and the secondary image (solid line) of a star lensed by Sgr A* in the black-hole scenario. The star is moving along a trajectory 200 pc behind Sgr A* with the impact L=2 mpc. The distance to Sgr A* is assumed to be 8 kpc. The (x,y) projection of the star trajectory is shown by the horizontal dashed line. The Einstein ring is represented by the dashed circle. The dotted line represents the continuation of the secondary image trajectory corresponding to the part of the trajectory of the primary image that goes outside the boundaries of the plot.

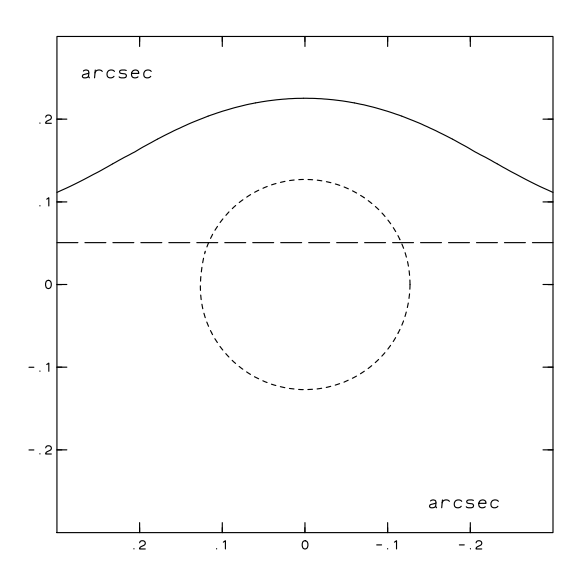


Fig. 5.— Trajectory of the image (solid line) of a star lensed by Sgr A* in the fermion-star scenario. The star is moving along a trajectory 200 pc behind Sgr A* with the impact L=2 mpc. The (x,y) projection of the star trajectory is shown by the horizontal dashed line. The Einstein ring is represented by the dashed circle.

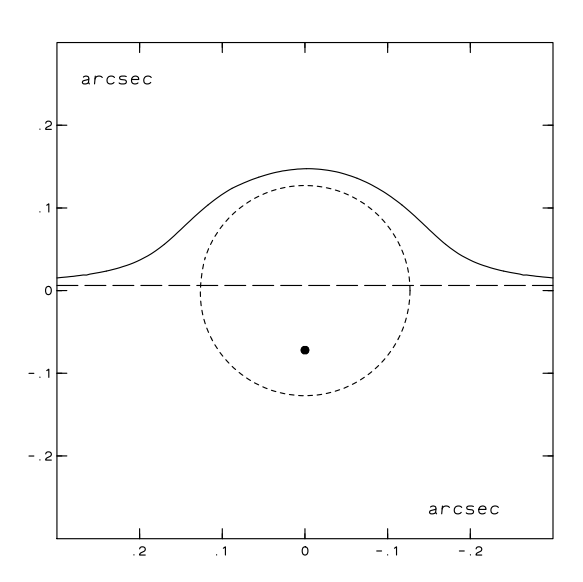


Fig. 6.— Same as in Figure 5, with L=0.2497 mpc. The dot inside the Einstein ring represents a degenerated trajectory loop of the two secondary images.

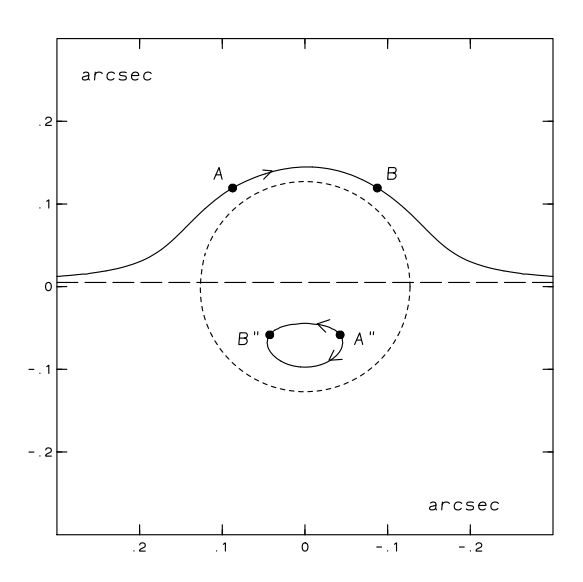


Fig. 7.— Same as in Figure 5, with L=0.2 mpc. The secondary images appear at the point A'' and disappear at B''.

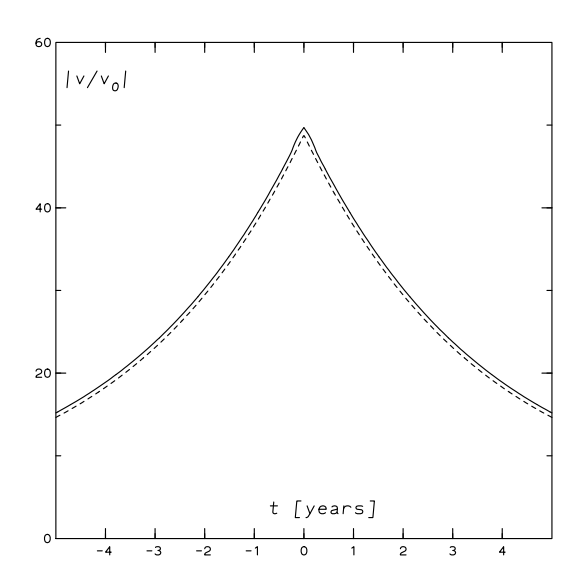


Fig. 8.— Velocity of the primary (solid line) and the secondary (dashed line) image divided by the velocity of the star, for lensing by a black hole as in Figure 4 with L=0.2 mpc.

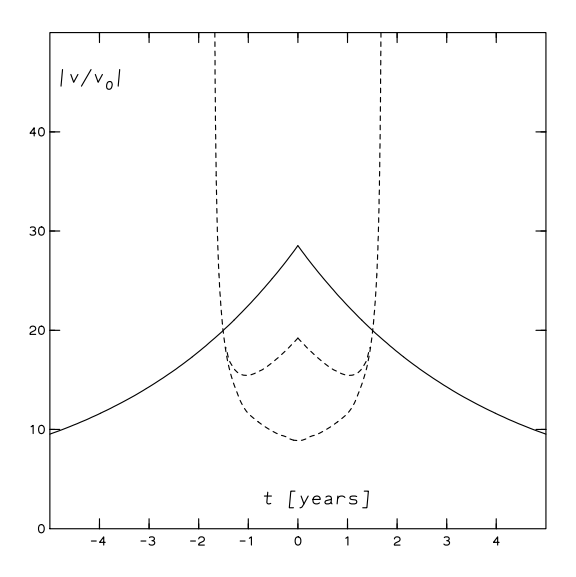


Fig. 9.— Velocity of the primary (solid line) and the secondary (dashed line) images divided by the velocity of the star, for lensing by a fermion star as in Figure 7.

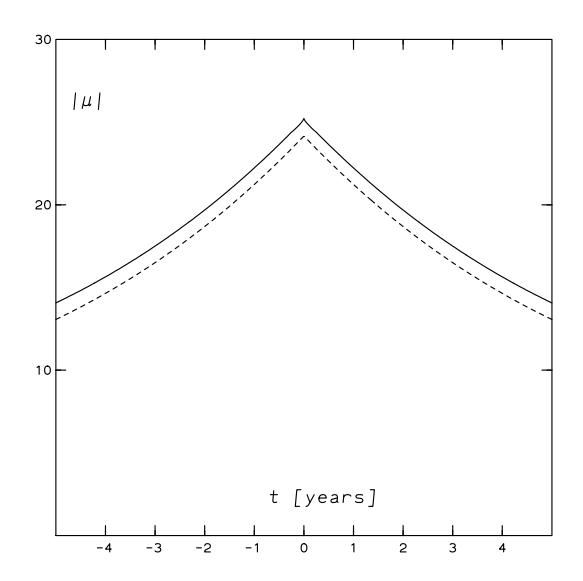


Fig. 10.— Magnification of the primary (solid line) and the secondary (dashed line) image as a function of time for lensing by a black hole as in Figure 4 with L=0.2 mpc.

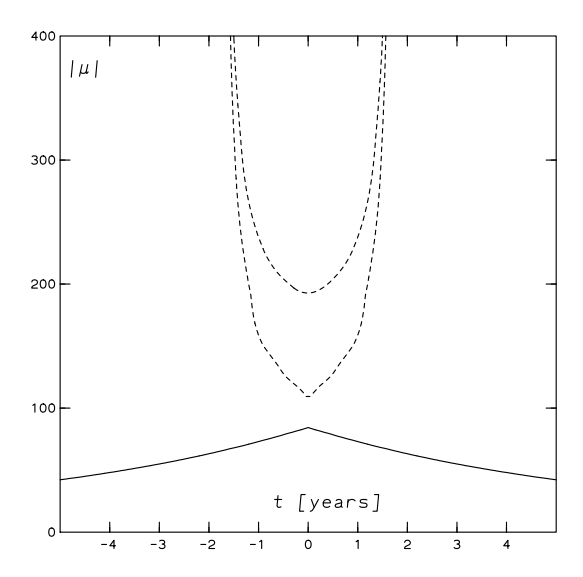


Fig. 11.— Magnification of the primary (solid line) and the secondary (dashed line) images as a function of time for lensing by a fermion star as in Figure 7.

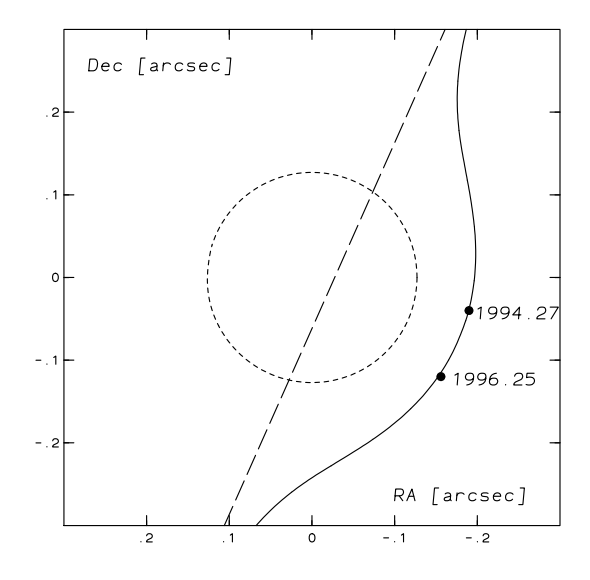


Fig. 12.— Trajectory of the image (solid line) of S1 lensed by Sgr A* assuming the fermion-star scenario. The star is moving along a trajectory (dashed line) 205 pc behind Sgr A* with the impact L=1 mpc. The Einstein ring is represented by the dashed circle.

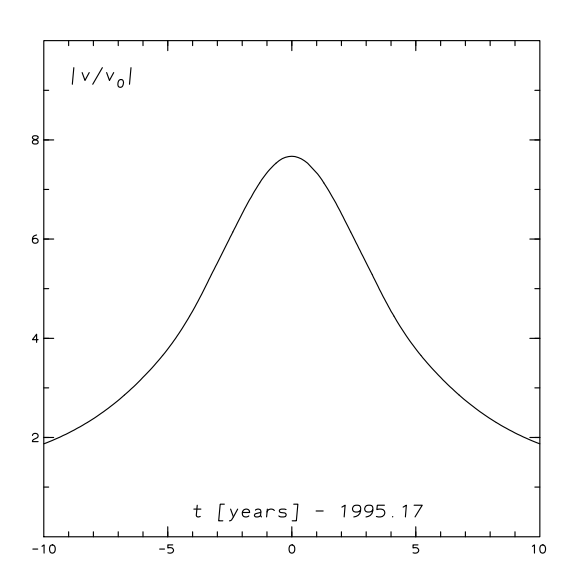


Fig. 13.— Ratio of the image velocity of S1 to the velocity of the star as a function of time.